AUTHOR MANUSCRIPT

Publication details:	Gangoda L, Schenk RL, Best SA, Nedeva C, Louis C, D'Silva DB, Fairfax K, Jarnicki AG, Puthalakath H, Sutherland KD, Strasser A, Herold MJ. Absence of pro-survival A1 has no impact on inflammatory cell survival in vivo during acute lung inflammation and peritonitis. *Cell Death and Differentiation.* 2022 29(1):96-104
Final authenticated version Is available online at:	https://doi.org/10.1038/s41418-021-00839-3

Absence of pro-survival A1 has no impact on inflammatory cell survival *in vivo* during acute lung inflammation and peritonitis

Lahiru Gangoda[1,2,3], Robyn L. Schenk[1,2], Sarah A. Best[1,2], Christina Nedeva[3], Cynthia Louis[1,2], Damian B. D'Silva[1,2], Kirsten Fairfax[1,2,4], Andrew G. Jarnicki[5], Hamsa Puthalakath[3], Kate D. Sutherland[1,2], Andreas Strasser[1,2] and Marco J. Herold*[1,2]

[1] The Walter and Eliza Hall Institute of Medical Research (WEHI), 1G Royal Parade, Parkville, Melbourne, Victoria 3052, Australia

[2] Department of Medical Biology, University of Melbourne, Parkville, Melbourne, Victoria 3010, Australia

[3] La Trobe Institute for Molecular Science, La Trobe University, Melbourne, VIC, 3086, Australia

[4] Menzies Institute for Medical Research, University of Tasmania, Hobart, Tasmania, Australia

[5] Department of Biochemistry and Pharmacology, University of Melbourne, Parkville, Victoria, Australia

* Correspondence to: Marco J. Herold, The Walter and Eliza Hall Institute of Medical Research, 1G Royal Parade, Parkville, Victoria 3052, Australia. Tel: +61 3 9345 2497 or +61 3 9345 2555; Fax: +61 3 9347 0852; E-mail: herold@wehi.edu.au

Abstract

Inflammation is a natural defense mechanism of the body to protect against pathogens. It is induced by immune cells, such as macrophages and neutrophils, which are rapidly recruited to the site of infection, mediating host defense. The processes for eliminating inflammatory cells after pathogen clearance are critical in preventing sustained inflammation, which can instigate diverse pathologies. During chronic inflammation, excessive and uncontrollable activity of the immune system can cause extensive tissue damage. New therapies aimed at preventing this over-activity of the immune system could have major clinical benefit. Here, we investigated the role of the pro-survival Bcl-2 family member A1 in the survival of inflammatory cells under normal and inflammatory conditions using murine models of lung and peritoneal inflammation. Despite the robust upregulation of A1 protein levels in wild-type cells upon induction of inflammation, the survival of inflammatory cells was not impacted in *A1*-deficient mice compared to wild-type controls. These findings indicate that A1 does not play a major role in immune cell homeostasis during inflammation and therefore does not constitute an attractive therapeutic target for such morbidities.

Introduction

Inflammation is an important innate immune response which is usually activated by the ligation of pattern recognition receptors (PRRs) leading to upregulation of a broad range of pro-inflammatory factors, including cytokines and chemokines, and migration of leukocytes from the circulation to the site of tissue damage [1]. The clearance of these cells, once the infection or injury have been resolved, is crucial for the tissue healing process. An acute inflammatory response lasts only a few days, whilst a response of longer duration is referred to as chronic inflammation.

B-cell lymphoma 2 (BCL-2) family of proteins are the critical regulators of the intrinsic apoptotic pathway [2]. However, A1 (in humans called BFL-1), remains a relatively poorly characterised anti-apoptotic protein [3]. *BCL2A1* (encoding A1) was first identified as an early response gene induced in bone marrow derived macrophages in response to treatment with granulocyte macrophage colony stimulating factor (GM-CSF) and lipopolysaccharide (LPS). This study also demonstrated that in mice, A1 expression is restricted to cells of the haematopoietic compartment [3]. In humans BFL-1 expression appears to be more widespread, but it is still predominantly found in haematopoietic cells [4]. A1/BFL-1 expression can be induced by inflammatory cytokines, such as tumour necrosis factor alpha (TNFα*)* and IL-1β [5]. The identification of *BCL2A1* as an NF-kB target gene [6] and its expression in inflammatory cells suggest a role for A1 during inflammation.

In mice, studies of A1 are complicated by the prescence of three functional isoforms (A1-a, -b, - and -d) and a pseudogene (A1-c) [7]. Mice lacking the *A1-a* isoform displayed only minor defects in neutrophils and mast cells [8, 9]. Recently we generated mice lacking all three

functional isoforms of A1 (*A1*$^{-/-}$ mice) and found that they do not display any major abnormalities [10]. Here, we utilised *A1*$^{-/-}$ mice to assess an *in vivo* role of A1 in response to specific inflammatory challenges.

Neutrophils in the blood are the first line defence against an infection. They are continuously released from their bone marrow reservoir, into the blood and are recruited to sites of infection. Circulating neutrophils have a short lifespan of only ~7 h in the absence of infection [11]. This cellular lifespan is extended after exposure to GM-CSF, granulocyte-colony stimulating factor (G-CSF) or diverse pathogen or damage associated molecular patterns, such as LPS [12, 13]. Prolonged neutrophil survival and activity can be detrimental and their death is required for resolution of inflammation [14].

The limited lifespan of neutrophils is partly due to their expression of pro- and anti-apoptotic proteins. Mcl-1 is critical for neutrophil survival under steady state [15]. Human neutrophils also express other anti-apoptotic proteins, including BFL-1 [16]. Similar to Mcl-1, A1 is also a short-lived pro-survival protein [17, 18]. Here, we examined the role of A1 in neutrophil survival in mouse models of inflammation *in vivo.*

Results

A1 protein is strongly upregulated upon pro-inflammatory stimuli *in vivo*.

A1 protein expression was analysed by Western blotting of lung tissues and peritoneal lavage cells from wild-type (WT) and A1 knockout (*A1*$^{-/-}$) mice that had been challenged with the indicated inflammatory stimuli using our recently developed monoclonal antibody[19]. Intranasal administration of LPS or *Pseudomonas aeruginosa* (PA) significantly upregulated A1 expression in the lungs of WT mice (Fig. 1a and 1b). Similarly, A1 expression was

induced in the peritoneal cells of WT mice following intraperitoneal (i.p.) injection of LPS or caecal slurry (CS) containing bacteria (Fig. 1a and 1b). The spleen and bone marrow were used as distal organ controls (Fig. 1a). LPS and many other constituents from bacteria stimulate PRRs which lead to the activation of NF-kB signalling and hence, the upregulation of A1 expression. A1 expression was either absent or very low in the lung, spleen, peritoneal cells and bone marrow of naïve mice and was only increased in the bone-marrow in response to LPS (Fig. 1a). We also assessed A1 expression following non-microbial stimuli using the monosodium urate (MSU)-induced peritonitis or ovalbumin (OVA)-induced lung inflammation models. This revealed robust induction of A1 in both settings (Fig. 1c).

A1 has been shown to be important in regulating neutrophil survival *in vitro* [20, 21]. Western blot analysis of isolated neutrophils from the lungs of LPS treated mice confirmed a marked upregulation of A1 in the enriched neutrophil fraction (Supplementary Fig. S1). Collectively, these findings demonstrate that A1 is induced in neutrophils upon pro-inflammatory stimuli.

The absence of A1 does not impact neutrophil survival during LPS induced lung inflammation

Given the upregulation of A1 expression in inflammatory neutrophils *in vivo* in response to inflammatory insults, we tested whether A1 is critical for neutrophil survival in this setting. Upon intranasal challenge of LPS, the lungs of both WT and *A1*$^{-/-}$ mice contained increased immune cell infiltration compared to PBS-treated controls, demonstrating successful induction of lung inflammation (Fig. 2). Immune cell composition of lung tissues was further analysed by flow cytometry at 24 h post-challenge. No major differences was observed in the frequencies or numbers of B cells, T cells, macrophages or neutrophils in the lungs of WT and *A1*$^{-/-}$ mice (Fig. 2 and Supplementary Fig. S2) following LPS challenge or PBS control

treatment. Gating strategy used for flow cytometry analysis of immune cells is shown in Supplementary Fig. S3. These results demonstrate that A1 is dispensable for survival of lung-infiltrating immune cells during inflammation. LPS challenge, however, significantly reduced the number of lung B cells in both WT and *A1*$^{-/-}$ mice compared to PBS-treated mice. While we do not understand the nature of this decrease, similar observations have been made in lung cancer models [22].

We also examined the immune cell composition of lung tissues at earlier time point (4 h post LPS challenge) by flow cytometry (Supplementary Fig. S4). Again, no major difference was observed in the frequencies or numbers of T cells, macrophages or neutrophils in the lungs of WT and *A1*$^{-/-}$ mice at 4 h post-challenge. At this early time point, there were more B cells in LPS induced *A1*$^{-/-}$ lungs in comparison to WT lungs. This difference was no longer seen at the 24 h timepoint with no impact in the overall inflammatory response (Fig. 2). Inflammatory cytokines in the bronchoalveolar lavage fluid (BALF) were assessed by ELISA at 4 h following intranasal instillation of LPS. Interestingly, the levels of TNF and GM-CSF were significantly lower in the BALF of *A1*$^{-/-}$ mice compared to WT mice at 4 h post-LPS challenge (Supplementary Fig. S5).

A1 deficiency causes a minor reduction in neutrophils during *Pseudomonas aeruginosa* induced lung inflammation

The murine pulmonary PA infection model closely mimics bacterially-induced pneumonia in humans. Mice were intranasally administered with PA ($\sim 1.5 \times 10^7$ CFU) to induce lung inflammation. Infected animals initially lose weight and show neutrophil-induced acute lung inflammation as the bacterial infection is rapidly cleared [23, 24]. At 24 h post-infection, the lungs were analysed by flow cytometry to identify the infiltrating haematopoietic cell subsets.

Infection with PA induced an influx of neutrophils (Fig. 3) and the frequencies of lung neutrophils from infected *A1*$^{-/-}$ mice were significantly lower than those seen in infected WT mice (Fig. 3). Observation at 24 h post-infection revealed similar weight loss but worse body condition in the *A1*$^{-/-}$ mice (Supplementary Fig. S6 a). In other mouse inflammatory models, (e.g. LPS, *Mycobacterium bovis*-derived Bacillus Calmette-Guerin (BCG), or *Toxoplasma gondii)* A1 is transiently upregulated during the first 8–16 h and at 24 h the levels of A1 is again reduced [25, 26, 27]. Therefore, we conducted these experiments within the 24 h time frame.

The clearance of the bacteria from the lungs was examined by flow cytometric analysis for internalised bacteria in granulocytes (Gr-1^{+}) (Supplementary Fig. S6 b). Additionally, colony formation assays of lung extracts of PA-infected mice were performed to determine the number of bacteria (Supplementary Fig. S6 c). These assays did not show any difference in bacterial clearance between *A1*$^{-/-}$ and WT mice 24 h post-infection (Supplementary Fig. S6 b and c).

A1 is not required for the accumulation of neutrophils during caecal slurry or LPS induced peritonitis

Polymicrobial sepsis was induced in mice by i.p. injection of caecal contents of laboratory animals into test animals [28]. We assessed the onset of clinical signs, including reduced motor activity, lethargy, shivering, piloerection, rapid shallow breathing and also measured the systemic levels of inflammatory cytokines.

We first determined the optimal concentration of CS to induce acute sepsis in mice. Doses below 0.5 g/kg were non-lethal to mice at 24 h post-injection (Supplementary Fig. S7 a and b). In separate survival studies, mice were injected with lethal doses (>0.5 g/kg) of CS (Fig.

4). We hypothesised that differences in neutrophil survival between WT and *A1*$^{-/-}$ mice would result in a difference in bacterial clearance and, consequently, in animal survival. Injection of 0.75 g/kg or 1 g/kg CS caused severe morbidity requiring euthanasia within 18-24 h in 100% of both WT and *A1*$^{-/-}$ mice. Treatment with 0.55 g/kg CS caused severe disease in 28% and 43% of WT and *A1*$^{-/-}$ mice, respectively, within 48 h. Injection of 0.65 g/kg CS necessitated euthanasia of 38% and 88% of WT and *A1*$^{-/-}$ mice, respectively, at 48 h (Fig. 4). Despite these differences in survival at 48 h with 0.55 g/kg and 0.65 g/kg doses, the overall difference between survival curves did not reach statistical significance because animals of the two genotypes showed similar survival at later time points. Neutrophil mobilisation from the bone marrow was observed at the minimum non-lethal dose of CS tested (0.2 g/kg), but there was no difference between the WT and *A1*$^{-/-}$ mice (Supplementary Fig. S8 a and b).

The peritoneal lavage, blood and bone marrow were obtained at 4 h and 18 h post-CS (0.65 g/kg) injection for flow cytometric analysis (Fig. 5 a and Supplementary Fig. S9). Although at 4 h there were no obvious differences in the different haematopietic cell populations between WT and *A1*$^{-/-}$ mice, by 18 h there were some differences, albeit minor (Fig. 5 a and Supplementary Fig. S9). In the peritoneum of WT and *A1*$^{-/-}$ mice, the percentages of neutrophils increased and the percentages of T cells and macrophages decreased at 4 h post-CS injection.

As an additional model of peritoneal inflammation, we injected mice i.p. with LPS (1 mg/kg). Cells from the peritoneal lavage and blood were analysed by flow cytometry at 4 h post-injection. There were no differences in cell subset composition between WT and *A1*$^{-/-}$ mice injected with LPS. However, there was a significantly reduced frequency of peritoneal macrophages in PBS injected *A1*$^{-/-}$ mice compared to their WT counterparts (Fig. 5 a). There

was an increase in the percentages of neutrophils and a decrease in the percentages of lymphocytes in the blood of both WT and *A1*$^{-/-}$ mice upon i.p. injection of LPS (Supplementary Fig. S10).

Increased infiltration of neutrophils to the site of infection may result in higher levels of inflammatory cytokines. Inflammatory cytokines in the peritoneal lavage were assessed by ELISA following injection of CS. The levels of TNF were slightly higher in *A1*$^{-/-}$ mice at 4 h, and the levels of IL-1β were slightly lower in *A1*$^{-/-}$ mice at 18 h (Fig. 5 b). Furthermore, we analysed the degree of cell death in the peritoneal cells during CS- and LPS-induced peritonitis (Supplementary Fig. S11). Following induction of inflammation, both WT and *A1*$^{-/-}$ cells underwent increased apoptosis compared to their PBS injected counterparts but there were no significant differences between the level of cell death between the WT and *A1*$^{-/-}$ mice within each treatment.

No redundancy between A1 and other pro-survival proteins in the LPS induced lung inflammation model and peritonitis model

Neutrophils are highly sensitive to Fas-induced apoptosis [12]. The FasL–Fas induced apoptotic pathway also plays a role in the death of other immune cells, including B cells and T cells [29]. It has previously been reported that A1 delays spontaneous and Fas ligand-induced apoptosis of activated neutrophils [21] and B cells [30]. Hence, one possible reason we did not observe a significant defect in neutrophils or B cells in our experiments with *A1*$^{-/-}$ mice could be due to the compensatory role of other pro-survival proteins. Our data suggest that the role of A1 in regulating immune cell survival during an inflammatory response may be redundant and may only becomes prominent in the absence of additional pro-survival proteins.

To investigated this possibility, we used the LPS-induced lung inflammation model in compound mutant mice that lack not only A1 but also lack one allele of a gene for an additional pro-survival BCL-2 family member (i.e. *A1*$^{-/-}$*;Bcl-X*$^{+/-}$, *A1*$^{-/-}$*;Bcl-2*$^{+/-}$ and *A1*$^{-/-}$*;Mcl*$^{+/-}$). Partial loss of the other pro-survival proteins in addition to complete absence of A1 did not lead to increased death of any of the immune cell sub-types tested (Supplementary Fig. S12). The lack of effect seen in these heterozygous compound mutants may be due to the the fact that these proteins are still present albeit at a reduced level. Because homozygous deficiency of MCL-1, BCL-XL and BCL-2 is embryonic lethal in mice [31, 32, 33], we performed ex vivo studies using BH3 mimetics [34, 35] to block MCL-1, BCL-XL and BCL-2. We collected peritoneal lavage cells from WT and *A1*$^{-/-}$ mice that were injected with with LPS 4 h prior and cultured these cells with BH3 mimetics [34, 35] . There were no differences in the rate of cell death between WT and *A1*$^{-/-}$ cells in the presence of BH3 mimetics, which indicate no redundancy between A1 and other pro-survival proteins (Supplementary Fig. S13).

Discussion

Neutrophils are key players during inflammation. Neutrophil apoptosis during resolution of inflammation is necessary for their subsequent engulfment by macrophages [36]. We observed a strong upregulation of the pro-survival protein A1 during pathogen-induced inflammation, both in the lungs and the peritoneal cavity of challenged mice. We further showed that A1 levels were increased in neutrophils and hypothesised that this increase in A1 protects neutrophils from premature apoptosis, thereby extending their lifespan.

We therefore investigated the role of A1 in regulating neutrophil survival during inflammatory responses *in vivo*. We confirmed the upregulation of A1 in neutrophils in the lungs and peritoneal cavity during inflammation, but suprisingly, our findings indicate that

A1 does not have a major role in regulating neutrophil survival at sites of inflammation. This is despite an interesting observation in which we detected lower levels of TNF and GM-CSF in the BALF of *A1*$^{-/-}$ mice at 4h post LPS challenge. Alveolar macrophages have been shown as a key producer of TNF during lung inflammation that in turn promotes GM-CSF upregulation and secretion from the lung epithelium[37]. The overall lung macrophage numbers in *A1*$^{-/-}$ mice are comparable to WT mice before and after LPS treatment, which indicate that the reduction in TNF and GM-CSF levels in the inflamed lung of *A1*$^{-/-}$ mice was not due to an underlying defect in macrophage numbers. We also observed no major impact on immune cell mobilization/recruitment, pathogen clearance or inflammatory cell survival in response to diverse stimuli in *A1*-deficient animals.

Observations in *A1*-deficient mice during inflammation may not truly reflect the role of its homologue BFL-1 in humans. There are several differences between mouse A1 and human BFL-1. Mice have four *A1* genes (three expressed, one pseudo-gene), whereas humans only have one *BCL2A1* gene [7]. These gene duplication events may have occurred and been preserved in evolution because different A1 proteins have designated roles in different tissues in mice [3]. In mice, A1 expression is restricted to cells of the haematopoietic compartment [3], while in humans BFL-1 expression is more widespread [4].

Although neutrophils appear to express similar levels of all three functional A1 genes [7], differential expression of these isoforms has been observed in other cell types. For example, A1-b is reported to be the predominant form expressed in thymocytes as well as in resting T cells and B cells. A1-a seems the least abundant isoform but one study reported its upregulation, alongside A1-d, upon TCR ligation in $CD8^+$ T cells [38, 39]. Mouse A1 proteins are preferentially localised in the cytosol, whereas human BFL-1 can be found on the outer

mitochondrial membrane. However, there is evidence that the pro-survival functions of A1 and BFL-1 may be independent of their sub-cellular localisation, at least when overexpressed at high levels [17, 40].

The balance of lymphocytes and neutrophils is rather different between humans and mice: human blood is neutrophil rich (~70% neutrophils, ~30% lymphocytes), whereas mouse blood has a strong preponderance of lymphocytes (~75% lymphocytes, ~25% neutrophils) [41, 42]. If A1/BFL-1 is required for neutrophil survival during inflammation, the functional consequences of its absence may be more prominent in humans.

The LPS induced murine lung inflammation model accurately mimics the neutrophilic inflammatory response seen in humans [43]. Administration of free-living PA to the murine lung results in either rapid bacterial clearance or acute overwhelming sepsis depending on the functionality of the immune system of the treated mouse [44].

We modeled human intra-abdominal inflammation by using both LPS and CS i.p. injections. LPS injection represents a model that is simple to use and highly reproducible [45] where the host responds to bacterial products rather than the pathogen itself. There is a marked difference in the response to LPS between species. Rodents are relatively resistant to LPS, whereas humans and non-human primates show more profound responses [45]. Compared to treatment with LPS, in the murine CS model, injection of free-living bacteria into mice promotes a lower but longer lasting increase in the levels of pro-inflammatory cytokines with more accurate manifestation of the pathological changes that occur in human sepsis [46, 47].

Despite the several models of inflammation used, we could not establish evidence for a critical involvement of A1 during inflammation. We could also not establish an overlapping function with other and likely more dominant pro-survival proteins, such as Mcl-1. Therefore, A1 is not an attractive therapeutic target for the treatment of inflammatory diseases.

Acknowledgements

We acknowledge the invaluable contributions of the animal caretaker staff for animal husbandry and the flow cytometry facility of WEHI.

Funding Statement

This work was supported by grants and fellowships from the Australian National Health and Medical Research Council (NHMRC) (Project Grants 1186575, 1159658 and 1145728 to MJH, 1143105 to MJH and AS), Program Grant 1016701 to AS and Fellowships 1020363 to AS, 1156095 to MJH), the Leukemia and Lymphoma Society of America (LLS SCOR 7015-18 to AS and MJH), the Cancer Council of Victoria (project grant 1147328 to MJH, 1052309 to AS and Venture Grant to MJH and AS), the Australian Phenomics Network (to MJH), the Leukaemia and Lymphoma Society Grant #7001-13 to AS; the estate of Anthony (Toni) Redstone OAM and The Craig Perkins Cancer Research Foundation; and operational infrastructure grants through the Australian Government NHMRCS IRIISS and the Victorian State Government Operational Infrastructure Support to AS and the CASS Foundation Science and Medicine Grant #9393 to LG. KF is the recipient of the Alex Gadomski Fellowship, funded by Maddie Riewoldt's Vision. KDS is supported by the Peter and Julie Alston Cententary Fellowship.

Author contributions

L.G. performed and designed most experiments and wrote the manuscript; R.L.S., S.A.B., C.N., C.L., D.D. and K.F. helped to perform experiments and write the manuscript; A.J. H.P. and K.D.S. helped with discussions and advice on neutrophil experiments and write the manuscript; A.S. and M.J.H. planned the project, were involved in experimental design and helped write the manuscript.

Conflict of interest

The authors declare that they have no conflict of interest.

Ethics Statement

All animal experiments were approved by the Walter and Eliza Hall Institute of Medical Research (WEHI) and the La Trobe University (LTU) Animal Ethics Committees.

Methods

Mice

The generation of *A1*$^{-/-}$ mice has been described previously [10]. All mouse strains have been generated on and were maintained on a C57BL/6 background and equal proportions of 7 to 8 week-old males and females were used in all experiments. The mice were transported and

housed short term under specific pathogen-free conditions at the La Trobe Animal Research and Training Facility (LARTF) for PA and CS experiments. Except for the PA and CS experiments all other experiments were performed at WEHI.

Intranasal injection of LPS

Mice were slightly anaesthetised with Methoxyflurane. Anaesthetised mice received intranasal instillation of 10 μg of LPS and control mice received an equivalent volume of PBS. The mice were placed under a heat lamp or on a heat pad and were monitored until fully conscious.

Intranasal administration of *Pseudomonas aeruginosa*

Pseudomonas aeruginosa ATC27853 strain was grown overnight in 5 mL of LB broth. The bacteria were spun down and resuspended in PBS to obtain an OD_{600} of 0.7. Mice were anaesthetised (as described above) and administered with 40 μL of the solution containing PA ($\sim 1.5 \times 10^7$ CFU) or 40 μL of PBS.

Induction of acute polymicrobial sepsis

The CS injection method was used to induce polymicrobial sepsis. In brief, 50 naive wild-type adult C57BL/6 mice were euthanised and 10 g of ceacal content was harvested. The caecal content was resuspended in 5% dextrose to obtain a CS stock of 250 mg/mL, which was then filtered through a 100 μm filter. This stock was aliquoted, stored and used for all CS experiments to prevent batch variations. Mice were injected with 0.1 mg/kg Buprenorphine 30 min before CS injection. Mice were i.p. injected with CS and monitored every 3 h up to

first 72 h and then twice a day up to 2 weeks. Mice were euthanised if signs of distress were observed.

Induction of inflammation by non-microbial components

For the gout model, 2 mg of MSU crystals dissolved in PBS were i.p. injected into mice and peritoneal lavage was obtained 16 h post-injection for Western blotting. For the acute asthma model, a suspension containing 20 ug ovalbumin (OVA) and 2.25 mg aluminium hydroxide was injected i.p. into mice on day 1 and day 14, and mice were aerosol challenged either with PBS or OVA for 15 min per day on days 21, 22 and 23. 24 h after the last exposure, mice were euthanised and organs harvested.

Harvesting of cells from mice

Mice were euthanised by CO_2 asphyxiation. For bone marrow retrieval, the femur was flushed with 1 mL of PBS buffer. Cells were passed through a 100 μm cell strainer to obtain a single-cell suspension. For blood cell analysis, bleeds were taken into Microvette tubes containing anti-coagulants from mice immediately following euthanasia. For obtaining cells from the peritoneal cavity, mice were i.p. injected with 5 mL of cold PBS immediately following CO_2 asphyxiation and gently massaged. The lavage containing the cells was drawn back into the syringe and the cells were then recovered by centrifugation. Peritoneal cells were subjected to flow cytometric analysis and the lavage fluid was used to measure cytokine levels by ELISA according to the manufacturer's instructions (eBioscience).

For obtaining the bronchoalveolar lavage fluid (BALF) for cytokine ELISA, lungs were flushed with 0.3 mL of PBS twice. A total of 0.5-0.6 mL lavage were obtained from each

392 mouse and were subsequently spun to pellet the cells. The BALF supernatant was subjected
393 to cytokine analysis by ELISA. Pellleted BALF cells were pooled with the cells obtained
394 from whole lung digestion. Lung tissues were minced, and tissue dissociation was carried out
395 by enzymatic digestion (in medium containing 0.2 g/L glucose and 20 mg/mL Worthington
396 Collagenase Type 1) as previously described [48]. All processed cell pellets requiring red blood
397 cell lysis were resuspended in red cell lysis buffer (0.156 M NH_4Cl) and left at 25 °C for
398 5 min. The supernatant was removed, and the cells were resuspended in FACS buffer (PBS
399 with 2% fetal calf serum) and stained with appropriate antibodies.
400
401 **Neutrophil isolation**
402 Neutrophils were isolated from the pellet of cells resulting from the processed lungs by using
403 the Stem Cell Technologies' Mouse Neutrophil Enrichment Kit according to the
404 manufacturer's instructions.
405
406 ***P. aeruginosa* colony formation assay**
407 The left lobe of the lung was dissected and homogenised in 1 mL of PBS. 20 µL of the
408 suspension was dropped onto an LB agar plate as the undiluted sample. Subsequent dilutions
409 were carried out in PBS and 20 µL from each of these dilutions was also dropped onto LB
410 agar plates. Plates were incubated overnight at 37 °C and visible bacterial colonies were
411 counted on the following day.
412
413 **Western blotting**
414 Total protein extracts were prepared by lysing cells in lysis buffer (20 mM Tris-pH 7.4,
415 135 mM NaCl, 1.5 mM $MgCl_2$, 1 mM EGTA, 10% (v/v) glycerol and 1% (v/v) Triton-X-100;
416 Sigma-Aldrich) with complete protease inhibitor cocktail (Roche) for 1 h at 4 °C. Equal

amounts of protein were electrophoresed on NuPAGE 4–12% Bis Tris gels (Invitrogen) before transferring to nitrocellulose membranes (Life Technologies) and probing with primary antibodies: monoclonal rat anti-mouse A1 (clone 6D6, WEHI antibody facility), monoclonal-mouse anti-HSP70 (clone N6, W. Welch USCF). Secondary anti-rat (#3010-05)/anti-mouse (#1010-05) IgG antibodies conjugated to HRP (Southern BioTech, Birmingham, AL, USA) were applied, followed by Luminata Forte Western HRP substrate (Millipore, Billerica, MA, USA) for band visualisation. Membranes were imaged using the ChemiDoc XRS+ machine with ImageLab software (Bio-Rad). Quantification of the Western blot band intensities was carried out using the Fiji Image J software.

Statistical analysis

Data are presented as the mean ± s.e.m. Unpaired two-tailed student's *t*-test and *P* values were used to determine statistical significance. *P* values < 0.05 were considered as statistically significant, and *P* values > 0.05 were considered non-significant. T-tests were corrected for multiple testing by controlling the false discovery rate. For mouse survival data analysis, the significance was calculated using the log-rank test (Prism Software, Graphpad). The variance was similar between statistically compared experimental groups. Either one-way or two-way analysis of variance (ANOVA) was used based on the experimental design.

Haematopoietic cell analysis and flow cytometry

Peripheral blood was analysed with the ADVIA automated haematology system (Bayer). Lung, bone marrow and peritoneal lavage cell populations were examined using flow cytometry. Cell populations were identified by staining with fluorochrome-conjugated monoclonal antibodies (produced in-house or purchased from BioLegend) that detect cell subset specific surface markers: B220 (BV605)) (#103243, Biolegend), TCRβ (PE-Cy7)

(#109222, Biolegend), MAC-1 (FITC), GR-1 (APC) and Ly5.2 (PE). Dead cells were excluded from analysis by staining with propidium iodide (PI, 5 μg/mL). To determine the intracellular PA, cells were fixed and permeabalised using eBioscience intracellular fixation and permeabilisation buffer set and stained with Rabbit anti-*Pseudomonas* antibody (#ab68538, Abcam) followed by a FITC-conjugated anti-rabbit IgG secondary antibody. Flow cytometry was performed on the LSR II flow cytometer (BD Biosciences) and data were analysed using FlowJo software (FlowJo LLC).

References

1. Takeuchi O, Akira S. Pattern recognition receptors and inflammation. *Cell* 2010, **140**(6)**:** 805-820.

2. Yip KW, Reed JC. Bcl-2 family proteins and cancer. *Oncogene* 2008, **27**(50)**:** 6398-6406.

3. Vogler M. BCL2A1: the underdog in the BCL2 family. *Cell Death Differ* 2012, **19**(1)**:** 67-74.

4. Lin EY, Orlofsky A, Berger MS, Prystowsky MB. Characterization of A1, a novel hemopoietic-specific early-response gene with sequence similarity to bcl-2. *J Immunol* 1993, **151**(4)**:** 1979-1988.

5. Karsan A, Yee E, Kaushansky K, Harlan JM. Cloning of human Bcl-2 homologue: inflammatory cytokines induce human A1 in cultured endothelial cells. *Blood* 1996, **87**(8)**:** 3089-3096.

6. Zong WX, Edelstein LC, Chen C, Bash J, Gelinas C. The prosurvival Bcl-2 homolog Bfl-1/A1 is a direct transcriptional target of NF-kappaB that blocks TNFalpha-induced apoptosis. *Genes Dev* 1999, **13**(4)**:** 382-387.

7. Hatakeyama S, Hamasaki A, Negishi I, Loh DY, Sendo F, Nakayama K*, et al.* Multiple gene duplication and expression of mouse bcl-2-related genes, A1. *Int Immunol* 1998, **10**(5)**:** 631-637.

8. Hamasaki A, Sendo F, Nakayama K, Ishida N, Negishi I, Nakayama K*, et al.* Accelerated neutrophil apoptosis in mice lacking A1-a, a subtype of the bcl-2-related A1 gene. *J Exp Med* 1998, **188**(11)**:** 1985-1992.

9. Xiang Z, Ahmed AA, Moller C, Nakayama K, Hatakeyama S, Nilsson G. Essential role of the prosurvival bcl-2 homologue A1 in mast cell survival after allergic activation. *J Exp Med* 2001, **194**(11)**:** 1561-1569.

10. Schenk RL, Tuzlak S, Carrington EM, Zhan Y, Heinzel S, Teh CE*, et al.* Characterisation of mice lacking all functional isoforms of the pro-survival BCL-2 family member A1 reveals minor defects in the haematopoietic compartment. *Cell Death Differ* 2017, **24**(3)**:** 534-545.

11. Summers C, Rankin SM, Condliffe AM, Singh N, Peters AM, Chilvers ER. Neutrophil kinetics in health and disease. *Trends Immunol* 2010, **31**(8)**:** 318-324.

12. O'Donnell JA, Kennedy CL, Pellegrini M, Nowell CJ, Zhang JG, O'Reilly LA*, et al.* Fas regulates neutrophil lifespan during viral and bacterial infection. *J Leukoc Biol* 2015, **97**(2)**:** 321-326.

13. Luo HR, Loison F. Constitutive neutrophil apoptosis: mechanisms and regulation. *Am J Hematol* 2008, **83**(4)**:** 288-295.

14. Koedel U, Frankenberg T, Kirschnek S, Obermaier B, Hacker H, Paul R*, et al.* Apoptosis Is Essential for Neutrophil Functional Shutdown and Determines Tissue Damage in Experimental Pneumococcal Meningitis. *Plos Pathogens* 2009, **5**(5).

15. Dzhagalov I, St John A, He YW. The antiapoptotic protein Mcl-1 is essential for the survival of neutrophils but not macrophages. *Blood* 2007, **109**(4)**:** 1620-1626.

16. Akgul C, Moulding DA, Edwards SW. Molecular control of neutrophil apoptosis. *FEBS Lett* 2001, **487**(3)**:** 318-322.

17. Herold MJ, Zeitz J, Pelzer C, Kraus C, Peters A, Wohlleben G*, et al.* The stability and anti-apoptotic function of A1 are controlled by its C terminus. *J Biol Chem* 2006, **281**(19)**:** 13663-13671.

18. Adams KW, Cooper GM. Rapid turnover of mcl-1 couples translation to cell survival and apoptosis. *J Biol Chem* 2007, **282**(9)**:** 6192-6200.

19. Lang MJ, Brennan MS, O'Reilly LA, Ottina E, Czabotar PE, Whitlock E*, et al.* Characterisation of a novel A1-specific monoclonal antibody. *Cell Death Dis* 2014, **5:** e1553.

20. Vier J, Groth M, Sochalska M, Kirschnek S. The anti-apoptotic Bcl-2 family protein A1/Bfl-1 regulates neutrophil survival and homeostasis and is controlled via PI3K and JAK/STAT signaling. *Cell Death Dis* 2016, **7:** e2103.

21. Schenk RL, Gangoda L, Lawlor KE, O'Reilly LA, Strasser A, Herold MJ. The pro-survival Bcl-2 family member A1 delays spontaneous and FAS ligand-induced apoptosis of activated neutrophils. *Cell Death Dis* 2020, **11**(6)**:** 474.

22. Best SA, De Souza DP, Kersbergen A, Policheni AN, Dayalan S, Tull D*, et al.* Synergy between the KEAP1/NRF2 and PI3K Pathways Drives Non-Small-Cell Lung Cancer with an Altered Immune Microenvironment. *Cell Metab* 2018, **27**(4)**:** 935-943 e934.

23. Kukavica-Ibrulj I, Levesque RC. Animal models of chronic lung infection with Pseudomonas aeruginosa: useful tools for cystic fibrosis studies. *Lab Anim* 2008, **42**(4)**:** 389-412.

24. Bayes HK, Ritchie N, Irvine S, Evans TJ. A murine model of early Pseudomonas aeruginosa lung disease with transition to chronic infection. *Sci Rep* 2016, **6:** 35838.

25. Kathania M, Raje CI, Raje M, Dutta RK, Majumdar S. Bfl-1/A1 acts as a negative regulator of autophagy in mycobacteria infected macrophages. *Int J Biochem Cell Biol* 2011, **43**(4)**:** 573-585.

26. Kausalya S, Somogyi R, Orlofsky A, Prystowsky MB. Requirement of A1-a for bacillus Calmette-Guerin-mediated protection of macrophages against nitric oxide-induced apoptosis. *J Immunol* 2001, **166**(7)**:** 4721-4727.

27. Orlofsky A, Somogyi RD, Weiss LM, Prystowsky MB. The murine antiapoptotic protein A1 is induced in inflammatory macrophages and constitutively expressed in neutrophils. *J Immunol* 1999, **163**(1)**:** 412-419.

28. Doerflinger M, Glab J, Puthalakath H. Experimental In Vivo Sepsis Models to Monitor Immune Cell Apoptosis and Survival in Laboratory Mice. *Methods Mol Biol* 2016, **1419:** 69-81.

29. Russell JH, Rush B, Weaver C, Wang R. Mature T cells of autoimmune lpr/lpr mice have a defect in antigen-stimulated suicide. *Proc Natl Acad Sci U S A* 1993, **90**(10)**:** 4409-4413.

30. Lee HH, Dadgostar H, Cheng Q, Shu J, Cheng G. NF-kappaB-mediated up-regulation of Bcl-x and Bfl-1/A1 is required for CD40 survival signaling in B lymphocytes. *Proc Natl Acad Sci U S A* 1999, **96**(16)**:** 9136-9141.

31. Rinkenberger JL, Horning S, Klocke B, Roth K, Korsmeyer SJ. Mcl-1 deficiency results in peri-implantation embryonic lethality. *Genes Dev* 2000, **14**(1)**:** 23-27.

32. Motoyama N, Wang F, Roth KA, Sawa H, Nakayama K, Nakayama K*, et al.* Massive cell death of immature hematopoietic cells and neurons in Bcl-x-deficient mice. *Science* 1995, **267**(5203)**:** 1506-1510.

33. Veis DJ, Sorenson CM, Shutter JR, Korsmeyer SJ. Bcl-2-deficient mice demonstrate fulminant lymphoid apoptosis, polycystic kidneys, and hypopigmented hair. *Cell* 1993, **75**(2)**:** 229-240.

34. Kotschy A, Szlavik Z, Murray J, Davidson J, Maragno AL, Le Toumelin-Braizat G*, et al.* The MCL1 inhibitor S63845 is tolerable and effective in diverse cancer models. *Nature* 2016, **538**(7626)**:** 477-482.

35. Merino D, Kelly GL, Lessene G, Wei AH, Roberts AW, Strasser A. BH3-Mimetic Drugs: Blazing the Trail for New Cancer Medicines. *Cancer Cell* 2018, **34**(6)**:** 879-891.

36. Cox G, Crossley J, Xing Z. Macrophage engulfment of apoptotic neutrophils contributes to the resolution of acute pulmonary inflammation in vivo. *Am J Respir Cell Mol Biol* 1995, **12**(2)**:** 232-237.

37. Cakarova L, Marsh LM, Wilhelm J, Mayer K, Grimminger F, Seeger W*, et al.* Macrophage tumor necrosis factor-alpha induces epithelial expression of granulocyte-

macrophage colony-stimulating factor: impact on alveolar epithelial repair. *Am J Respir Crit Care Med* 2009, **180**(6)**:** 521-532.

38. Verschelde C, Walzer T, Galia P, Biemont MC, Quemeneur L, Revillard JP*, et al.* A1/Bfl-1 expression is restricted to TCR engagement in T lymphocytes. *Cell Death Differ* 2003, **10**(9)**:** 1059-1067.

39. Tuzlak S, Schenk RL, Vasanthakumar A, Preston SP, Haschka MD, Zotos D*, et al.* The BCL-2 pro-survival protein A1 is dispensable for T cell homeostasis on viral infection. *Cell Death Differ* 2017, **24**(3)**:** 523-533.

40. Ottina E, Tischner D, Herold MJ, Villunger A. A1/Bfl-1 in leukocyte development and cell death. *Exp Cell Res* 2012, **318**(11)**:** 1291-1303.

41. Doeing DC, Borowicz JL, Crockett ET. Gender dimorphism in differential peripheral blood leukocyte counts in mice using cardiac, tail, foot, and saphenous vein puncture methods. *BMC Clin Pathol* 2003, **3**(1)**:** 3.

42. Mestas J, Hughes CCW. Of mice and not men: Differences between mouse and human immunology. *Journal of Immunology* 2004, **172**(5)**:** 2731-2738.

43. Wiener-Kronish JP, Albertine KH, Matthay MA. Differential responses of the endothelial and epithelial barriers of the lung in sheep to Escherichia coli endotoxin. *J Clin Invest* 1991, **88**(3)**:** 864-875.

44. Bragonzi A. Murine models of acute and chronic lung infection with cystic fibrosis pathogens. *Int J Med Microbiol* 2010, **300**(8)**:** 584-593.

45. Murando F, Peloso A, Cobianchi L. Experimental Abdominal Sepsis: Sticking to an Awkward but Still Useful Translational Model. *Mediators Inflamm* 2019, **2019:** 8971036.

46. Gonnert FA, Recknagel P, Seidel M, Jbeily N, Dahlke K, Bockmeyer CL*, et al.* Characteristics of clinical sepsis reflected in a reliable and reproducible rodent sepsis model. *J Surg Res* 2011, **170**(1)**:** e123-134.

47. Lee MJ, Kim K, Jo YH, Lee JH, Hwang JE. Dose-dependent mortality and organ injury in a cecal slurry peritonitis model. *J Surg Res* 2016, **206**(2)**:** 427-434.

48. Best SA, Kersbergen A, Asselin-Labat ML, Sutherland KD. Combining Cell Type-Restricted Adenoviral Targeting with Immunostaining and Flow Cytometry to Identify Cells-of-Origin of Lung Cancer. *Methods Mol Biol* 2018, **1725:** 15-29.

Figure Legends

Figure 1: A1 protein expression in tissues and cells upon induction of inflammation by microbial and non-microbial stimuli.

WT and A1 knockout (*A1*$^{-/-}$) mice were challenged with microbial components by either intranasal instillation or i.p. injection of **(a)** LPS, **(b)** *P. aeruginosa* (PA) or caecal slurry (CS). 24 h after LPS or PA treatments, lung tissues were harvested. Peritoneal lavage cells were harvested 4 h after LPS treatment and 18 h after CS treatment. **(c)** WT and *A1*$^{-/-}$ mice challenged with non-microbial components. Mice were i.p. injected with monosodium urate (MSU) crystals and peritoneal lavage was obtained at 24 h post injection. Mice were made to inhale Ovalbumin (OVA) and at the endpoint lung tissues were harvested. The lung and peritoneal lavage cells were analysed by Western blotting for A1 protein expression. Probing for HSP70 was used as a loading control.

Figure 2: Analysis of immune cell populations in the lungs during LPS induced inflammation.

WT and *A1*$^{-/-}$ mice were intranasally administered LPS (10 μg) or vehicle (PBS). After 24 h lung tissues were harvested and processed, and percentages of the indicated cell subsets were determined by flow cytometric analysis following staining for the indicated cell subset specific surface markers. Statistical significance (P* < 0.05, P** < 0.01) was determined using student's t-test. Each dot represents one mouse. The gating strategy used for flow cytometric analysis is shown in Supplementary Fig. S3. (n= 4-6 mice)

Figure 3: Analysis of the immune cell populations in the lungs during *P.aeruginosa* (PA) induced inflammation.

WT and *A1*$^{-/-}$ mice were intranasally administered *P. aeruginosa* (PA) or vehicle (PBS). After 24 h lung tissues were harvested and processed, and the percentages of the indicated cell subsets was determined by flow cytometric analysis following staining for the indicated cell subset specific surface markers. Statistical significance (P* < 0.05, P** < 0.01, P*** < 0.001) was determined using student's t-test. Each dot represents one mouse. The gating strategy used for flow cytometric analysis is shown in Supplementary Fig. S3. (n= 4 mice)

Figure 4: Kaplan–Meier curve presenting the survival of mice that had been injected with caecal slurry.

Groups of WT and *A1*$^{-/-}$ mice were injected i.p. with the indicated doses of caecal slurry and monitored every 3 h for up to 10 days and sacrificed when body condition scoring reached ethical endpoint. Overall survival graphs over the period of 10 days did not show any significant differences between WT and *A1*$^{-/-}$ mice at any of the doses (n= 3-8 mice).

Figure 5: Analysis of the immune cell populations in the peritoneal lavage of caecal slurry and LPS injected mice.

WT and *A1*$^{-/-}$ mice were injected i.p. with 0.65 g/kg caecal slurry (CS) or 1 mg/kg LPS. Mice were sacrificed at 4 h post-injection. **(a)** Percentages of the indicated cell subsets in the peritoneal lavage were determined at 4 h after CS or LPS injection by flow cytometric analysis following staining for the indicated cell subset specific surface markers. The gating strategy used for flow cytometric analysis is shown in Supplementary Fig. S3. **(b)** Serum levels of TNF, IL-1β and GM-CSF from mice undergoing polymicrobial sepsis were measured by ELISA 4 and 18 h after injection with CS. Statistical significance (P* < 0.05, P** < 0.01, P*** < 0.001) was determined using student's t-test. Each dot represents one mouse (n= 2-7 mice).

Figure 1

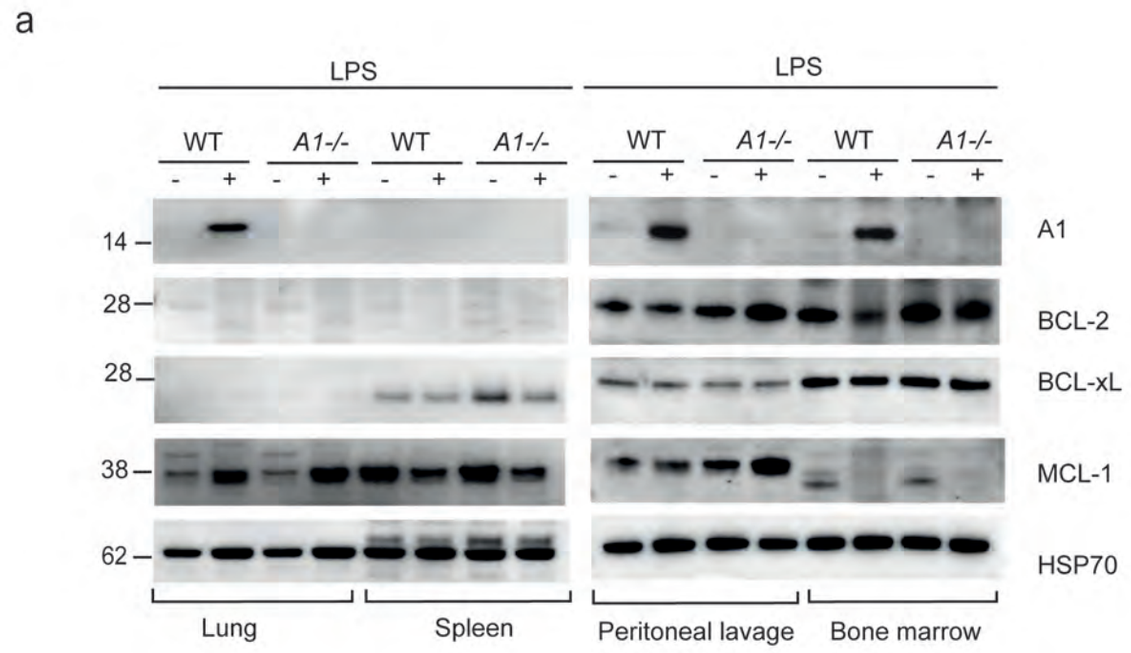
a
LPS
LPS
WT
A1-/-
WT
A1-/-
WT
A1-/-
WT
A1-/-
- + - + - + - + - + - + - + - + - +
14
28
28
38
62
A1
BCL-2
BCL-xL
MCL-1
HSP70
Lung
Spleen
Peritoneal lavage
Bone marrow

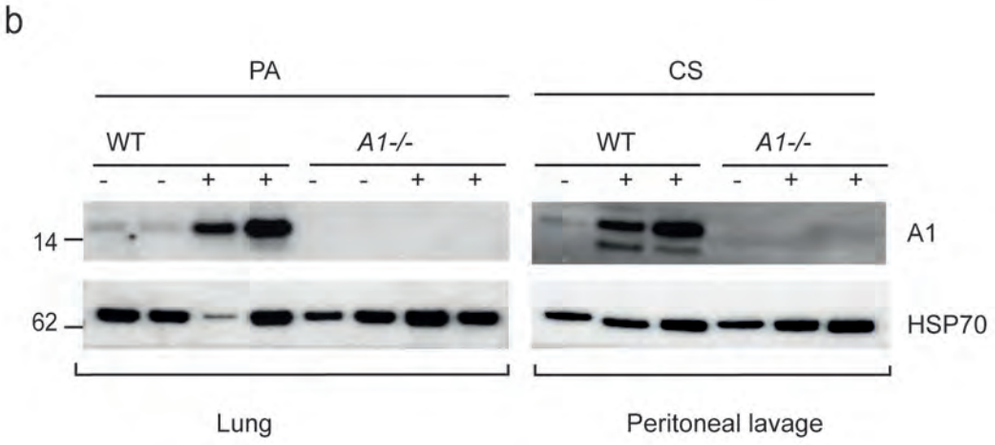
b
PA
CS
WT
A1-/-
WT
A1-/-
- - + + - - + + - + + - + + - +
14
62
A1
HSP70
Lung
Peritoneal lavage

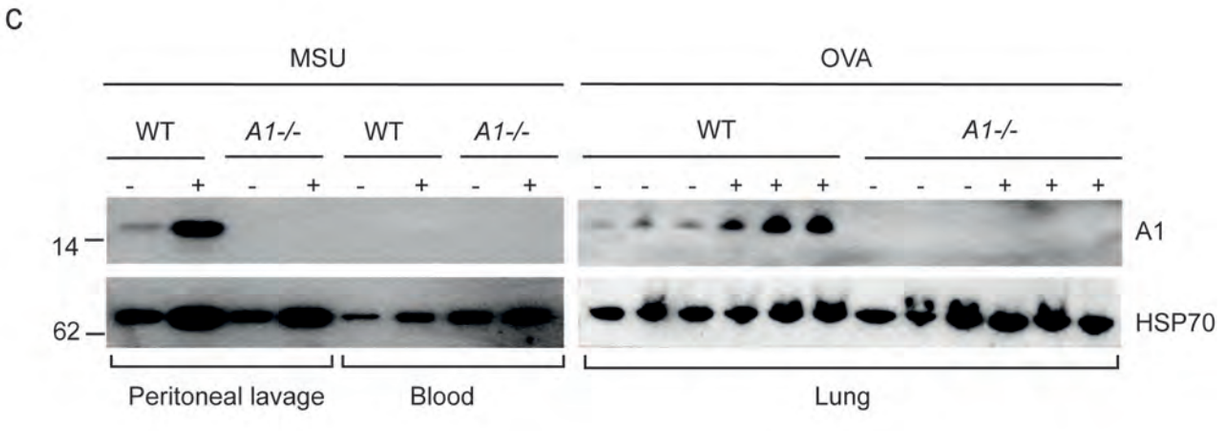
c
MSU
OVA
WT
A1-/-
WT
A1-/-
WT
A1-/-
- + - + - + - + - - - + + + - - - + + +
14
62
A1
HSP70
Peritoneal lavage
Blood
Lung

Figure 2

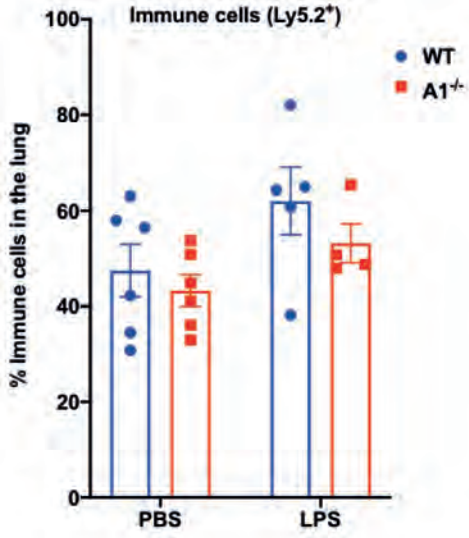
Immune cells (Ly5.2+)
% Immune cells in the lung
100
80
60
40
20
0
PBS
LPS
WT
A1-/-

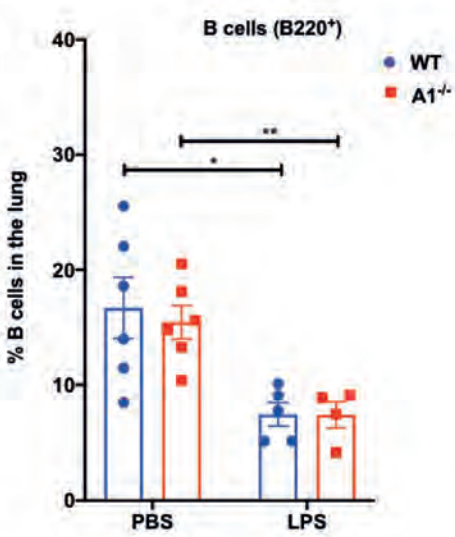
B cells (B220+)
% B cells in the lung
40
30
20
10
0
**
*
PBS
LPS
WT
A1-/-

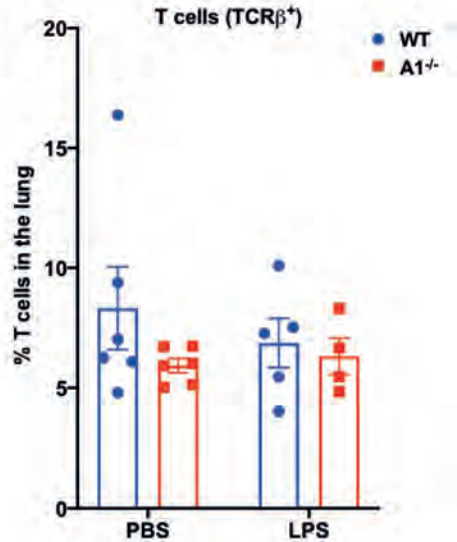
T cells (TCRβ+)
% T cells in the lung
20
15
10
5
0
PBS
LPS
WT
A1-/-

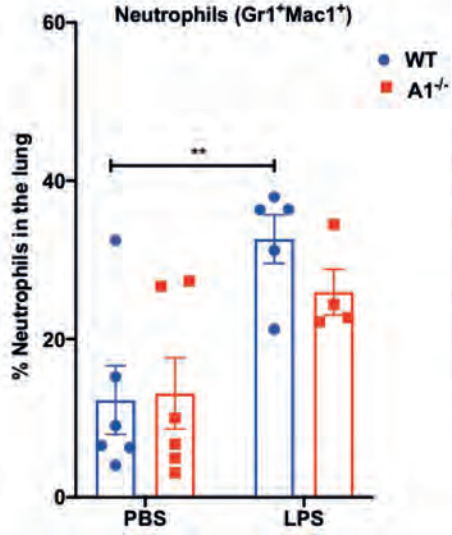
Neutrophils (Gr1+Mac1+)
% Neutrophils in the lung
60
40
20
0
**
PBS
LPS
WT
A1-/-

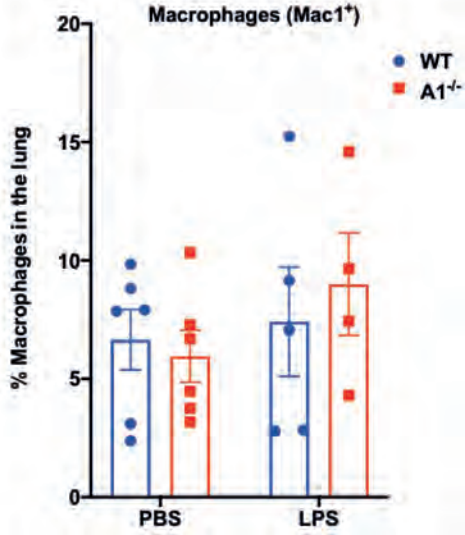
Macrophages (Mac1+)
% Macrophages in the lung
20
15
10
5
0
PBS
LPS
WT
A1-/-

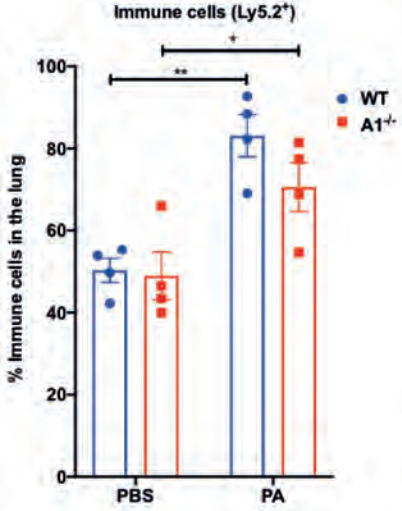
Immune cells (Ly5.2+)
% Immune cells in the lung
100
80
60
40
20
0
**
*
WT
A1-/-
PBS
PA

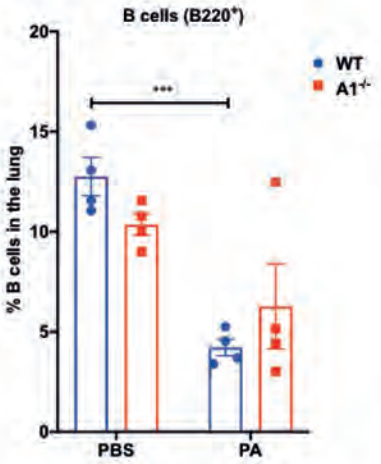
B cells (B220+)
% B cells in the lung
20
15
10
5
0
***
WT
A1-/-
PBS
PA

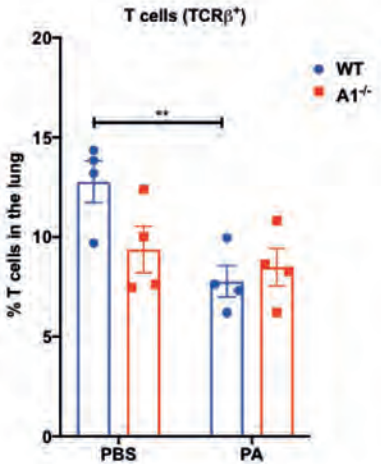
T cells (TCRβ+)
% T cells in the lung
20
15
10
5
0
**
WT
A1-/-
PBS
PA

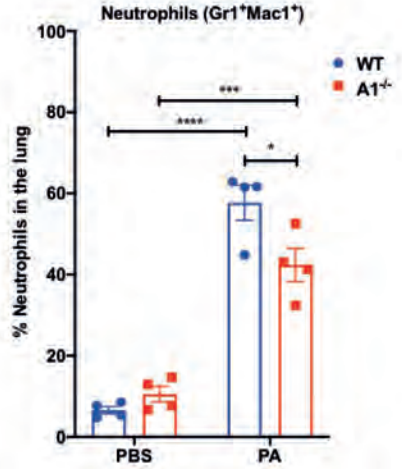
Neutrophils (Gr1+Mac1+)
% Neutrophils in the lung
100
80
60
40
20
0
***
****
*
WT
A1-/-
PBS
PA

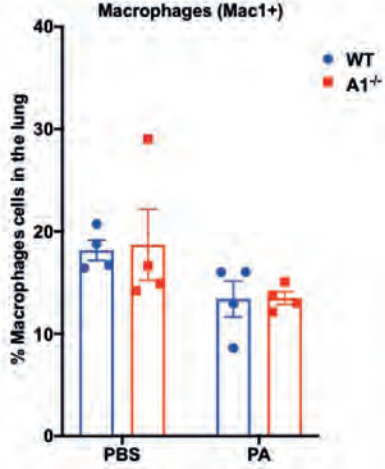
Macrophages (Mac1+)
% Macrophages cells in the lung
40
30
20
10
0
WT
A1-/-
PBS
PA

Figure 4

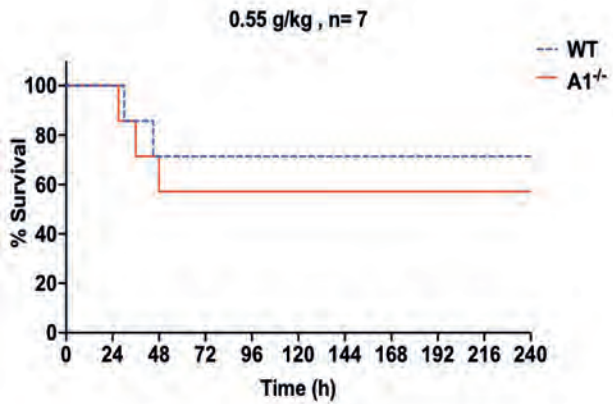
0.55 g/kg , n= 7
WT
A1-/-
% Survival
100
80
60
40
20
0
0 24 48 72 96 120 144 168 192 216 240
Time (h)

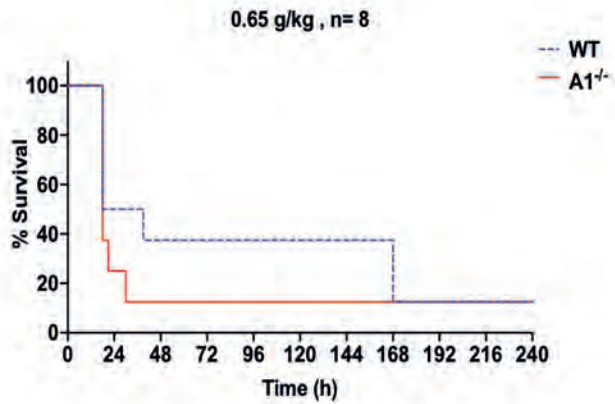
0.65 g/kg , n= 8
WT
A1-/-
% Survival
100
80
60
40
20
0
0 24 48 72 96 120 144 168 192 216 240
Time (h)

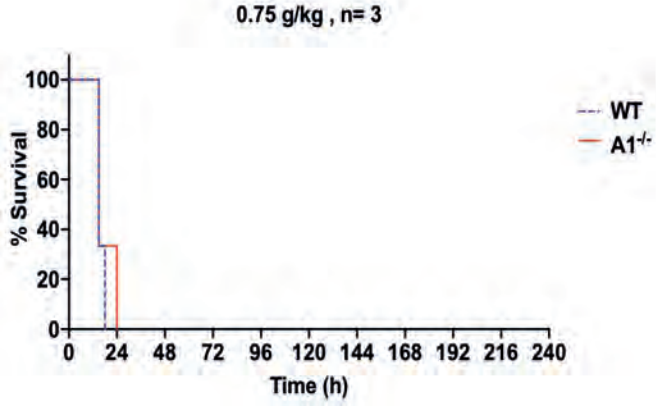
0.75 g/kg , n= 3
WT
A1-/-
% Survival
100
80
60
40
20
0
0 24 48 72 96 120 144 168 192 216 240
Time (h)

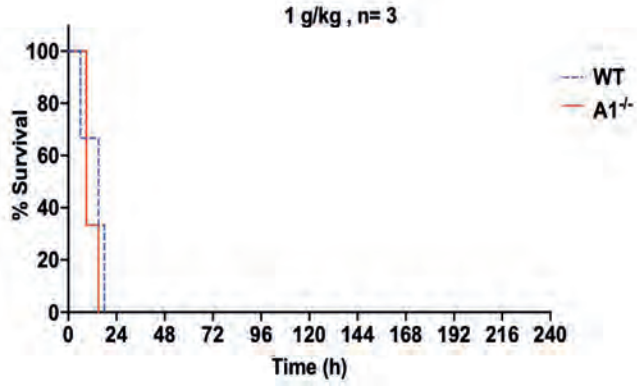
1 g/kg , n= 3
WT
A1-/-
% Survival
100
80
60
40
20
0
0 24 48 72 96 120 144 168 192 216 240
Time (h)

a

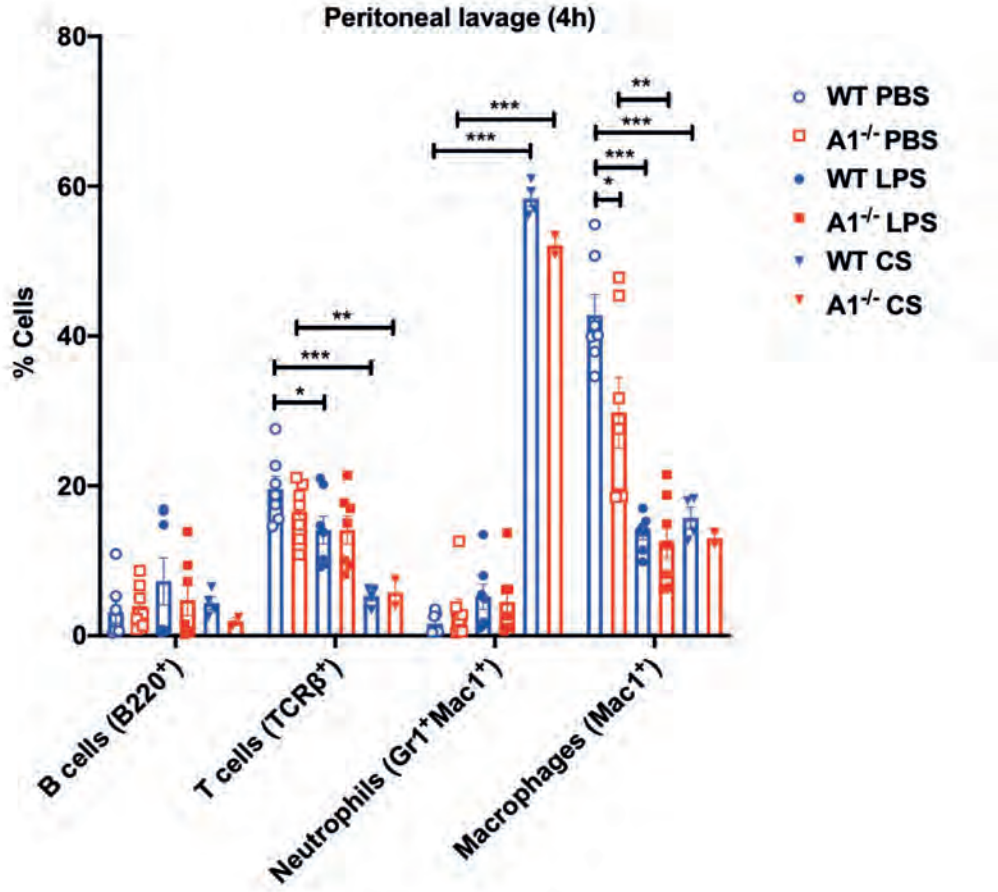
Peritoneal lavage (4h)
% Cells
80
60
40
20
0
WT PBS
A1-/- PBS
WT LPS
A1-/- LPS
WT CS
A1-/- CS
B cells (B220+)
T cells (TCRβ+)
Neutrophils (Gr1+Mac1+)
Macrophages (Mac1+)

b

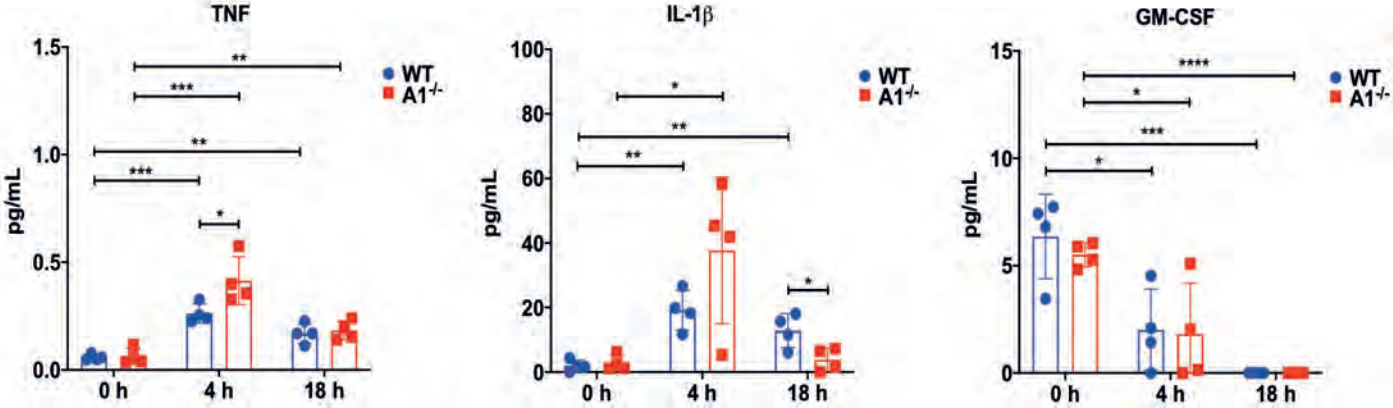
TNF
IL-1β
GM-CSF
pg/mL
WT
A1-/-
0 h
4 h
18 h